InSight Bulletin: A Multidisciplinary Interlink International Research Journal
Peer Reviewed International, Open Access Journal.
ISSN : 3065-7857 / Website: https://ibrj.us / Volume-3, Issue-5 / May - 2026

Original Article

Development of NiO-ZnO Nanocomposites Thick Film Sensors for the Detection of Hazardous Pollutants

Dr. Ujwala M. Pagar (Mhaske)
Department of Physics, HPT Arts & RYK Science College, Nashik,
Affiliated to SPPU, Pune M. S. India

Manuscript ID:
IBMIIRJ -2026-030502

Submitted: 09 Apr. 2026

Revised: 15 Apr. 2026

Accepted: 05 May 2026

Published: 31 May 2026

ISSN: 3065-7857

Volume-3

Issue-5

Pp. 11-20

May 2026

Correspondence Address:
Dr. Ujwala M. Pagar (Mhaske)
Department of Physics, HPT Arts & RYK Science College, Nashik, Affiliated to SPPU, Pune M. S. India
Email: ujwalapagar7@gmail.com

OPEN ACCESS

Quick Response Code:

Web. https://ibrj.us

DOI: 10.5281/zenodo.21637285

DOI Link:
https://doi.org/10.5281/zenodo.21637285

Abstract

The research concentrated on development of NiO-ZnO thick film sensors using standard screen-printed technique. The all films were prepared on glass substrate and characterized by several standard tools. The electrical characterizations was done using half bride method and static system. The structural, morphological and elemental analysis of the prepared thick film sensors were studied by X-ray diffractometer (XRD), Field Emission Scanning Electron Microscopy (FESEM) and EDAX technique respectively. The XRD plots was matched perfectly with JCPDS card No. 01-075-0197 and JCPDS card No. 00-036-1451 for NiO and ZnO respectively. Hexagonal Wurtzite structure of ZnO and Bunsenite face centred cubic (FCC) crystalline structure of NiO were confirmed from XRD analysis. FESEM results show that the surface of NiO-ZnO nanoparticles is smooth and uniform. The Brunauer-Emmett-Teller (BET) was analyzed for surface area and pore diameter parameters of the developed films. Energy dispersive analysis (EDAX) spectra shows presence of excess oxygen and non-stoichiometric nature of Ni, Zn and O. The developed NiO-ZnO nanocomposites thick films were utilized for application as a sensor for different pollutant gases like nitrogen dioxide (NO_2), ammonia (NH_3), ethanol (C_2H_5OH), and carbon dioxide (CO_2). The developed sensor shows the maximum sensitivity to nitrogen dioxide as compared to other tested gases. The sensitivity was found to be 76.18% at 100°C for a concentration of 500 ppm of nitrogen dioxide. ZnO doped NiO also shows quick response and recovery time.

Keywords: *Nanocomposites, screen-printed technique, additive, nitrogen dioxide, hazardous pollutants.*

Introduction

In recent decades, there has been a lot of interest in using detection sensing devices to improve environmental and safety monitoring of dangerous and combustible gases. Pollution, population, the development of harmful chemicals, poisonous gases generated by companies that lead to pollution, and genetic illnesses induced by pollution to the consumption of toxic substances are only a few of today's environmental challenges. The need of monitoring numerous dangerous and hazardous pollutants has escalated. This application's development needs the usage of reliable and low-cost gas sensors [1, 2].

Nanomaterials have gained in popularity in recent years due to the evolution of new techniques and processes. Using different synthesis techniques nanostructured metal oxides with different geometrical shapes have been developed [3, 4]. Because of their unique structure and various properties of nanomaterial have emerged as an advanced class of material science [5]. Nanocomposites are composites made up of at least two phases, one or both of which are nanoscale. Metal oxide nanoparticles and nanocomposites based on them are rapidly being used in a variety of applications. The use of heterojunctions to enhance the electrical, photovoltaic, optical, and gas sensing capabilities of nanostructured metal oxide composites has been widely used [6]. Nanotechnology is the framework for advancing our understanding of nanoscale materials and phenomena. Sensors are gaining a lot of interest since they can gather chemical information from the environment in real time, and as a result, they will have a growing impact on daily living [7]. Because nanoparticles increased optical emission and absorption due to electron movement from one state to another, nanodevice manufacture has considerably aided nanomaterials and nanotechnology research and development. Optoelectronic nanodevices benefit from this phenomenon [8, 9].

How to cite this article:
Pagar (Mhaske), U. M. (2026). Development of NiO-ZnO Nanocomposites Thick Film Sensors for the Detection of Hazardous Pollutants. InSight Bulletin: A Multidisciplinary Interlink International Research Journal, 3(5), 11–20. https://doi.org/10.5281/zenodo.21637285

Nickel oxide (NiO) films have a wide forbidden band gap [10]. NiO is a semiconductor from the group of transparent conductive oxides [11, 12]. NiO is a reversible magnetic compound [13] with a melting point of around 2000 °C, implying that it is durable and chemically stable. Solar cells, gas sensors, anti-reflection layers, laser mirrors, monochromatic filters, optoelectronics, and other applications of NiO are the most popular [12-15].

Zinc oxide (ZnO) is a transparent conductive oxide that belongs to the family of semiconductor chemical compounds known as transparent conducting oxides [16]. At ambient temperature, it has a wide band gap and an excitonic bonding energy of 60 MeV, making it ideal for sensing and optoelectronic device applications, gas sensors, ultrasonic devices, and other applications [16-18]. When diverse bandgap semiconductor metal oxide nano-materials are combined together to create nanocomposite, the physico-chemical characteristics are improved [19]. Zinc oxide is intrinsically n type and nickel oxide is a p-type semiconductor with a large direct bandgap of 3.37 eV and 3.6 eV respectively, the NiO-ZnO nanocomposite has gotten a lot of attention. The optical, electrical, gas sensing and electrochemical stability of ZnO and NiO are well reported [20-22].

In the present research work, the authors have focus on the development of NiO-ZnO nanocomposites thick film sensors on glass substrate by using screen printing technique. This present work focus on the study of electrical structural, and gas sensing properties of prepared NiO-ZnO thick film sensors.

Materials and Methods

1. Development of NiO-ZnO nanocomposites thick film sensors

In the current research work, commercially available AR grade (99.99 % purity) NiO and ZnO powder was used. For the preparation of NiO-ZnO nanocomposites thick films, NiO used as a functional material and ZnO as an additive. The ZnO was added in different weight percent proportions viz. 1 wt. %, 3 wt.%, 5 wt.%, 7 wt.% and 9 wt.% in the functional material NiO. The all films were prepared on a clean glass substrate. The distilled water and acetone were used to clean glass substrate. The 70 % inorganic (NiO-ZnO) and 30% organic material (ethyl cellulose and butyl carbitol acetate) composition was used for the preparation of films. Ethyl cellulose was used as a local binder and butyl carbitol acetate (BCA) was used for formation of thixotropic paste. The thixotropic paste was used to prepared thick films. By using standard screen printing set up thick films of NiO-ZnO were prepared. The prepared NiO-ZnO thick films were retained under IR lamp for 30 minutes to remove impurity residue, and then prepared films were used for further work.

2. Electrical characterization

The half-bridge approach was implemented to determine the DC resistance of the prepared films as a function of temperature. Eqs 1, 2, and 3 were used to determine the resistivity, activation energy, and temperature coefficient of resistance of the prepared thick films [2, 23].

$$\rho = \left(\frac{R \times b \times t}{l} \right) ohm - m \tag{1}$$

Where,

R= Resistance of the film at room temperature, t = thickness of the film, b = breadth of the film,

l = length of the film. $\Delta E = \frac{log\, R}{log\, Ro} \times KT$ (2)

Where, ΔE = Activation energy, R = Resistance at room temperature, R_0 = Resistance at room temperature, K = Boltzmann constant and T = Absolute temperature.

$$TCR = \frac{1}{R_o}\left(\frac{\Delta R}{\Delta T}\right) /^{O} K \tag{3}$$

Where, ΔR = change in resistance between temperature T_1 and T_2, ΔT = temperature difference between T_1 and T_2 and R_o = Resistance of the film at room temperature.

3. Structural Characterization The prepared NiO-ZnO nanocomposites thick films were characterised by XRD, FESEM, and EDAX to study the crystal structure, morphology, and elemental composition respectively. The thickness of the prepared films was calculated using the weight difference method.

X-Ray Diffraction

Using Rigaku diffractometer (DMAX-500), an X-ray diffractometer with CuKα radiation and wavelength (λ) = 0.154059 nm, XRD patterns of developed thick films were observed. The samples were examined between the range of 10° to 80°. The 2θ values obtained were compared to data files from the Joint Committee on Powder Diffraction Standards (JCPDS). Origin 9 software was used to calculate the full width of half maxima (FWHM). Debye Scherer's formula, Eq. 4, was used to determine the crystallite size [2].

$$D = \frac{K\lambda}{\beta Cos\theta} \tag{4}$$

Where, D= Crystallite size, K= Scherrer constant (0.9), β = Full width of half maxima (FWHM), and

λ =wavelength of X source.

FESEM and EDAX

The surface morphology of the developed thick films was characterized using a Field Emission Scanning Electron Microscope (FESEM) [Model JOEL 6300 LA GERMANY. Energy dispersive X-ray spectrometer (JEOL-2300, Germany) was used to do analysis the elemental compositions. The specific surface area calculated using FESEM images of developed thick films. The Eq.5, was used to estimate the specific surface area of thick films using the BET method for spherical particles [1, 23].

$$S_w = \frac{6}{\rho d} \tag{5}$$

Where Sw - Specific surface area, d - Diameter of the spherical particles, and ρ – Composite density.

Gas Sensing Characterization

Sensitivity, selectivity, reusability, response, and recovery time are all important performance characteristics for any gas sensors.

2.4.1 Sensitivity

A static gas sensing system was used to investigate the gas response of developed NiO-ZnO nanocomposites thick films. Nitrogen dioxide (NO_2), ammonia (NH_3), ethanol (C_2H_5OH), and carbon dioxide (CO_2) were used for the study of gas response. To determine gas response in the form of sensitivity, the electrical resistance of thick films in the air (Ra) and the presence of gas (Rg) were measured. The gas response or gas sensitivity was calculated by utilizing Eq. 6. [1, 2]

$$Sensitivity(\%) = \frac{\Delta R}{R_a} \times 100 \tag{6}$$

Where, Ra - Resistance of a thick film in air and Rg - Resistance of thick film presence of gas.

Selectivity

A sensor in a mixed gas atmosphere should only respond to one type of gas. The selectivity of a gas sensor towards a given gas is determined by the ratio of its reaction to that of another dominating interfering gas in the atmosphere. The selectivity of the developed NiO-ZnO nanocomposites thick films for a particular gas over others was determined using Eq.7 [23].

$$Selectivity\% = \frac{S_{gas}}{S_{target\,gas}} X100 \tag{7}$$

Where, S_{gas} = sensitivity of interfering gas at an optimum operating temperature and

$S_{target\ gas}$ = sensitivity of the target gas at the same temperature.

Reusability

Reusability is one of the most important indicators of sensor performance, along with stable baseline, regular response time, and recovery time, and it decides if the sensor can be operated in the real world rather than in the lab. The thick film sensor was tested five times with a 20-day gap between each cycle. The major goal of the reusability study was to see if the results of a NO_2 gas sensor could be reproducible. The reusability of the developed thick film sensor was investigated in the experiment [23].

Response and recovery time

When a sensor is exposed to a target gas, the response time is defined as the time it takes for it to attain 90% of its complete response, such as resistance. The time it takes for a sensor to return to 90% of its original baseline signal after the target gas has been removed is known as recovery time [2, 23].

Results and Discussion

Electrical Properties

1. Resistivity

The resistivity of the metal oxide semiconductor films is influenced by a number of factors including defects in crystal lattice, charge gradient surface defects and physical nonidealities, mainly roughness of the film and thickness of the films [24, 25]. The resistance of NiO-ZnO thick films were calculated by using half bridge method. Figure 1 reveals that the plot of resistance verses temperature of NiO-ZnO nanocomposites thick films. The resistance of NiO-ZnO films decreases as temperature increases, revealing that the films are semiconducting nature [1, 23]. The resistivity of NiO-ZnO thick films at 1 wt. %, 3 wt. %, and 5 wt. % were calculated 6283.38 Ω-m, 4773.09 Ω-m and 3823.94 Ω-m, respectively. It has been found that, the resistivity of NiO-ZnO thick films decreased as wt % additive (ZnO) increased. The resistivity of thick films decreases because of sufficient amount of NiO is present in compositional material. The ZnO particles are agglomerated around the NiO particles which would be forms the hetro p-n junction. The agglomeration of particle rise as wt % additive increases [26, 27].

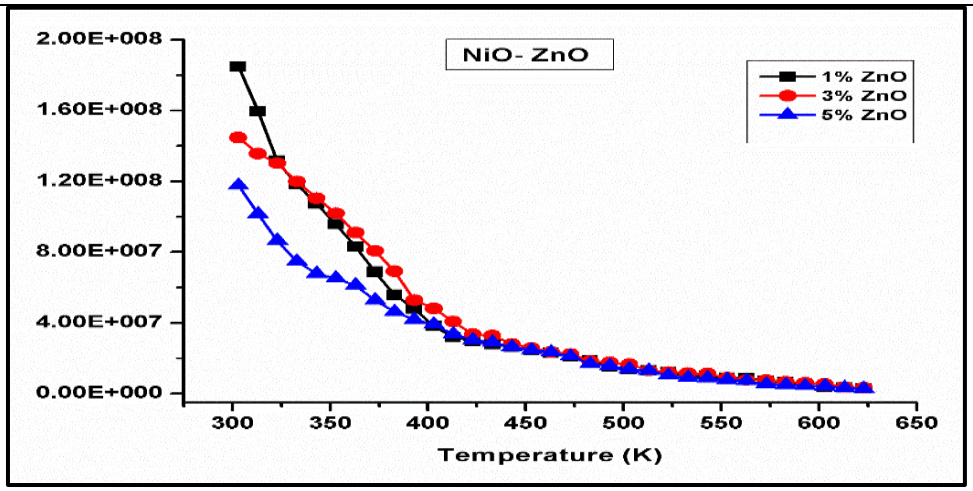

Fig. 1 Resistance verses temperature of NiO-ZnO nanocomposite thick films

2. Activation energy

The energy gap between Fermi level and bottom of the conduction band is equal to the electrical activation energy. As a result, the activation energy can be employed to determine Fermi level position [28, 29]. Using an Arrhenius plot for low and high temperature regions, the activation energy of the developed NiO-ZnO thick films was determined. The variation of log R versus the reciprocal of temperature (1/T) in NiO-ZnO thick films is depicted in Figure 2. The calculated activation at low and high temperature region tabulated in table1. The thickness of the films also decreases as the wt. % additive increases. The decrease in thickness of the prepared films causes the activation energy to increase, indicating that the semiconducting property is improving [27].

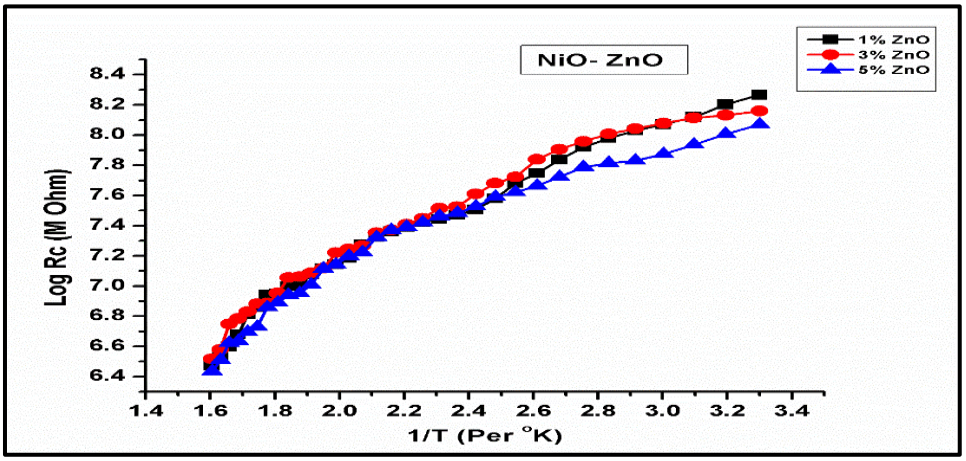

Fig. 2 Arrhenius plot of NiO-ZnO thick films

3. Temperature coefficient of resistance

The TCR of NiO-ZnO thick films was found to be -0.00611/° C, -0.00737 /° C, and -0.00641/° C at 1 wt. %, 3 and wt. %, 5 wt. % respectively. The negative sign indicates that the NiO-ZnO thick films have semiconducting properties [23]. Table 1 summarizes the electrical results of the NiO-ZnO thick films.

Table 1 Summary of electrical outcomes of NiO-ZnO nanocomposite thick films

Additive wt%.	Thickness (µm)	Resistivity (Ω.m)	TCR (/°C)	Activation Energy (eV)	
				At Low Temp x10⁻⁴	At High Temp x10⁻⁴
1% ZnO	68	6283.38	-0.00611	0.9772	5.2069
3% ZnO	66	4773.09	-0.00737	0.7843	2.8943
5% ZnO	65	3823.94	-0.00641	1.3766	8.3239

Structural properties

1. X-Ray Diffraction

Figure 3 shows the XRD pattern of NiO-ZnO thick films. The crystal structure of ZnO has found to be hexagonal Wurtzite structure while Bunsenite face centred cubic (FCC) crystalline structure for NiO. NiO patterns were observed, peaks were found at the diffraction angles: 2θ = 37.28°, 43.38°, and 62.94° corresponding to the Miller indices (111), (200), and (220), respectively. It is

seen that this sample possess preferred orientation along (200) plane. These lines are in a very good matching with those of JCPDS File no. 01-075-0197.

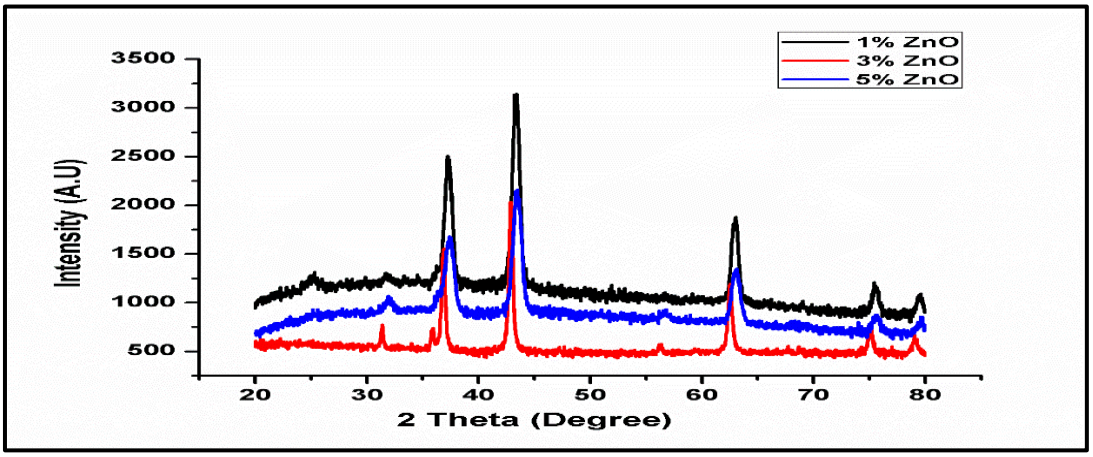

Fig.3 XRD pattern of NiO-ZnO thick films

ZnO patterns appeared at 2θ =34.48°, 36.28°, and 62.90° corresponding, respectively, (002), (101), and (103) orientations of hexagonal wurtzite structure with a preferential orientation along (002) peak according to the standard patterns (JCPDS File no. 00-036-1451) card [28]. As per structural analysis the crystallite size was calculated using Debye–Scherrer formula. The crystallite size (D) of NiO-ZnO thick films was found to be 11.71 nm, 10.20 nm and 9.35 nm for 1 wt. %, 3 wt. %, and 5 wt. % respectively. It has been observed that additive in wt % increases, the crystallite size of the films decreases. There is a reduction in the crystallite size from 11.71 to 9.35 nm. This behaviour can be ascribed to the changes in surface to volume ratios and surface areas of developed films. The decease crystallite size indicate more surface area, which is very helpful to gas sensing mechanism [29, 30]. The XRD results suggest that the NiO-ZnO nanocomposite is composed of crystalline NiO and ZnO nanostructures. Diverse structural parameters such as crystallite size, FWHM, dislocation density, and micro strain of NiO-ZnO thick films has been calculated. Table 2 illustrated the outcomes of structural parameters from XRD. From table 2, this is confirmed that the compatibility between the changes in micro strain and the dislocation density according to changes in the additive in wt %.

Table 2 Structural parameters from XRD of NiO-ZnO thick films

Additive wt%.	2θ(Degree)	FWHM	Crystallite size (nm)	Dislocation density (nm^{-2})	Micro strain ε (%)
1% ZnO	43.37	0.76278	11.71	7.292×10^{15}	0.0031
3% ZnO	42.91	0.38439	10.20	1.857×10^{15}	0.00156
5% ZnO	43.45	0.95628	9.35	11.43×10^{15}	0.00388

2. **Field Emission Scanning Electron Microscopy**

The FESEM tool was used to examine the morphology of developed NiO-ZnO nanocomposites thick films. Figure 4(a-c) depicts the surface morphology of films. Figure 4(a-c) depicted NiO-ZnO nanoparticles with a near round form. The round form nanoparticles are distributed randomly and amalgamated with ZnO. The penetration of ZnO into the NiO nanoparticle network was recently proved for similar NiO–ZnO nano heterojunctions [31, 32].

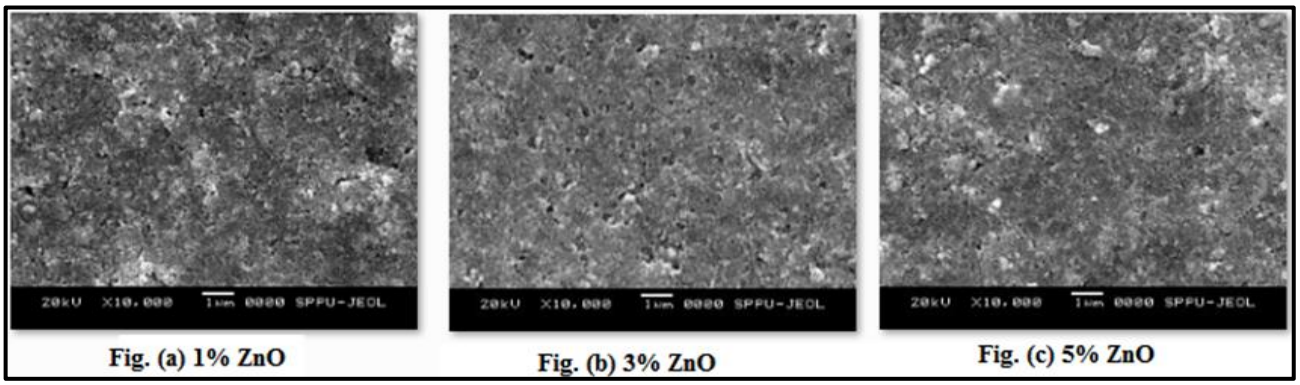

Fig.4 (a-c) FESEM micrographs of NiO-ZnO thick films

The surface of NiO-ZnO nanoparticles is smooth and homogeneous, with a small size distribution, as seen in FESEM images of NiO-ZnO thick films. FESEM micrographs also revealed an extremely porous structure. The growth of a very porous structure may occur as a result of additive effects. Some particles appear to be spherical in shape, and they are strongly agglomerated in figure 4(c).

The specific surface area of developed NiO-ZnO thick films was calculated by using Brunauer-Emmett-Teller (BET) method and image J software. The specific surface area of the NiO-ZnO thick films reveals in table 3. From table 3, it is clear that wt% of additive (ZnO) increases the specific surface area also increases, this result enhance the gas sensing properties of developed films.

Table 3 Outcomes form FESEM

Additive wt%.	Particle size (nm)	Specific surface area (m^2/g)
1% ZnO	245	3.493604
3% ZnO	146	5.881277
5% ZnO	103	8.363277

3. Energy dispersive analysis

Figure 5(a-c) shows the EDAX spectra of NiO-ZnO thick films. From Figure 5, it is clear that the film only contained Zn, Cu, and O according to the EDAX outcomes. Energy dispersive analysis (EDAX) spectra shows the film has oxygen excess and also shows that the presence of Ni, Zn and O are non-stoichiometry. It has been observed that the weight percentage of Zn is increased with increase additive in the NiO. The elemental composition of NiO-ZnO thick film were obtained from EDAX, clearly indicated the existence of nickel, zinc and oxygen with different atomic percentages with concentration of additive. From, EDAX plots, it confirmed that the atomic ratio of Ni/Zn in the resultant NiO–ZnO nanoparticles is well consistent with the composition.

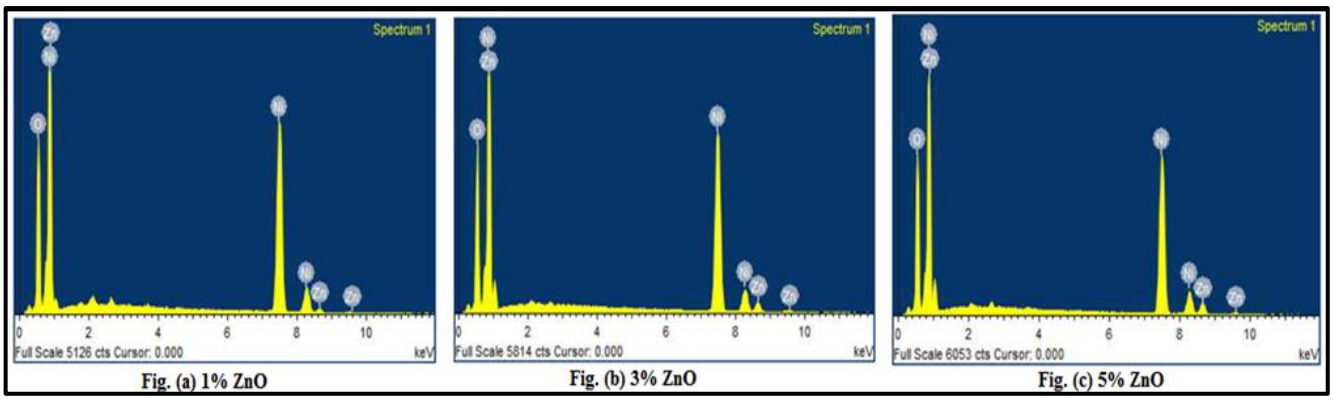

Fig. 5 (a-c) EDAX spectra of NiO-ZnO thick films

The mass percent and atomic weight percent of Zn, Ni, and O are nearly identical. From the EDAX spectra, it is found that atomic weight percentages of Ni, Zn, and O are nonstoichiometric. The atomic and weight percentages of analysis of film elements are tabulated in Table 3.

Table 3 Elemental composition of NiO-ZnO thick films

Additive wt%.	Element	Weight %	Atomic %
1% ZnO	Ni	58.25	28.42
	Zn	2.34	1.03
	O	39.41	70.56
3% ZnO	Ni	55.51	27.19
	Zn	5.28	2.32
	O	39.21	70.49
5% ZnO	Ni	52.91	25.59
	Zn	6.82	2.96
	O	40.27	71.45

Gas sensing study

The gas sensing performance of the developed NiO-ZnO nanocomposite thick films was investigated with the static gas sensing system. The entire developed thick film sensors viz. 1 wt. %, ZnO, 3 wt. % ZnO and 5 wt.% ZnO were investigated for several gas sensing parameters such as sensitivity, selectivity, reusability, response and recovery time as well as sensing mechanism of the gas sensors for the tested gases etc. The NiO-ZnO thick films has been used as a sensing element. At different working temperatures, the resistance of film was measured in the surrounding condition as well as targeted gaseous atmosphere with various ppm gas quantities.

1. **Sensitivity**

The effect of ZnO additive on NiO sensors was examined in this study at various concentrations of gas and operating temperature. Figure 6(a-c) shows the gas sensitivity of all concentrations (1 to 5 wt. %) of developed NiO-ZnO nanocomposite thick films. Figure 6 (a-c) illustrates the sensing response for various gases such as nitrogen dioxide, ammonia, ethanol, and carbon dioxide for ZnO doped NiO at fixed concentrations of 500 ppm. It is clear from all figures the maximum gas response was obtained for NO_2 gas at 100 °C among the other tested gases at a 5 wt. % NiO-ZnO thick film sensor. The effective specific surface area, optimum

porosity, and efficient ZnO additive over NiO lattice domain enhanced the various gas sensing and surface properties of the developed thick film sensor, resulting in the highest sensitivity for a 5 wt. % NiO-ZnO sensor. Sensitivity of the developed NiO-ZnO nanocomposite thick films was determined by using Eq. 6.

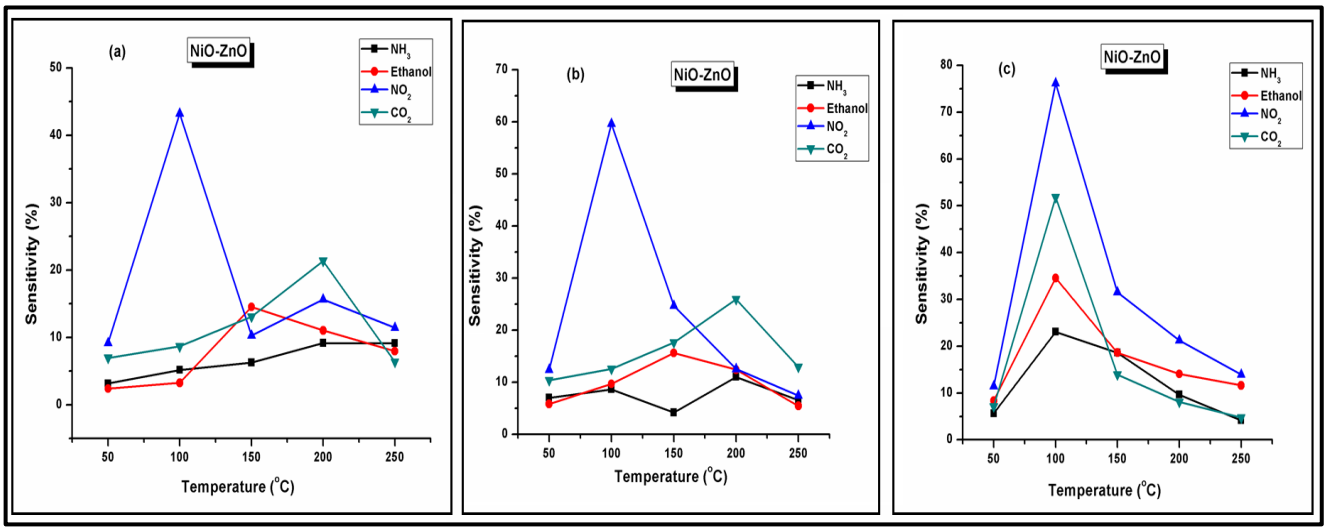

Fig. 6. (a) Sensitivity of 1 wt. %, ZnO-doped NiO for tested gases, (b) 3 wt. %, ZnO-doped NiO for tested gases, (c) 5 wt. %, ZnO-doped NiO for tested gases.

2. **Selectivity**

A successful gas sensor must be able to distinguish between different target gases. To determine the selectivity of a sensor for a certain target gas, an optimum working temperature was determined. Eq. 7 was used to determine the selectivity of developed NiO-ZnO nanocomposite thick films. The selectivity of the thick films for selected gases is shown in Figure 7.

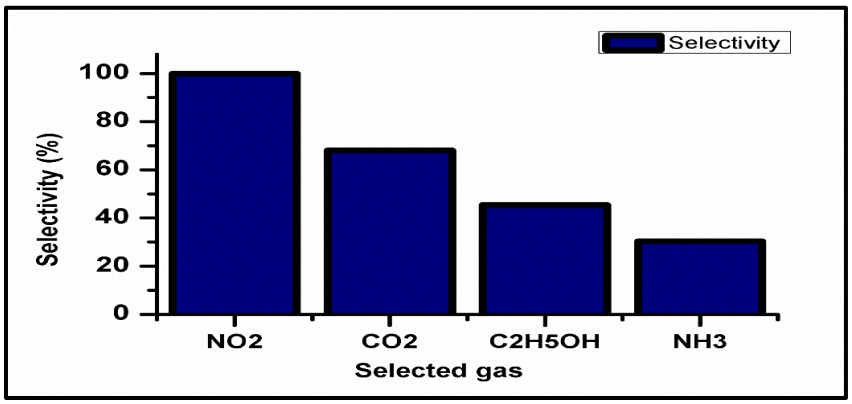

Fig. 7 Selectivity of developed NiO-ZnO nanocomposite thick films for selected gases at 150°C.

3. **Reusability**

One of the most essential characteristics for determining the long-term stability of sensors is reusability. Due to the frequent employment of metal oxide semiconductors base sensors, metal oxide semiconductors with drawbacks connected to sensor activity may be lessened or declined. As a result, the sensitivity of sensors has decreased [1, 23]. As a result, we examined the sensitivity of a 5 wt% doped NiO sensor by performing four gas sensing cycles/run over a period of 40 days with constant settings to ensure its stability. On developed NiO-ZnO nanocomposite sensors, we performed four cycles at 500 ppm of NO_2 gas. The graph for the developed sensor sensitivity reusability test is illustrated in Fig. 8. After a few days of consistent gas concentration, the gas reaction for all films was marginally reduced. All of the sensors showed very minor variation in sensitivity across four consecutive cycles with a 10-day interval, indicating that the sensors are stable over lengthy periods of time and repeated gas exposure.

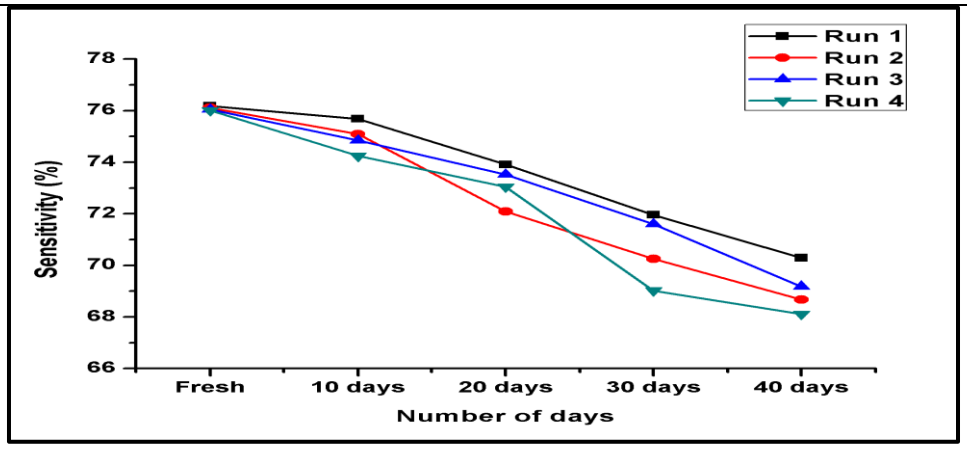

Fig. 8 Reproducibility results for NO_2 sensing at 500 ppm to 5 wt. % ZnO-doped NiO films

4. **Response and recovery time**

One of the crucial characteristics is response and recovery time for gas sensors. A typical sensor reaction time is the time it takes for a sensor to attain 90% of its peak incidence in conductance or decrease in resistance after being exposed to the target gas. A sensor's recovery time is the time it takes for it to restore to 90% of its initial resistance when the gas supply is cut off. The response and recovery for 5 wt. % ZnO-doped NiO films were recorded and shown in Fig. 8. The quick response time for NO_2 was 07 seconds, and the recovery time was 13 seconds. The fast response and recovery of sensors is attributable to the sensor's good morphology, which allows for quick and easy gas passage to grain boundaries, allowing for quick oxidation and response.

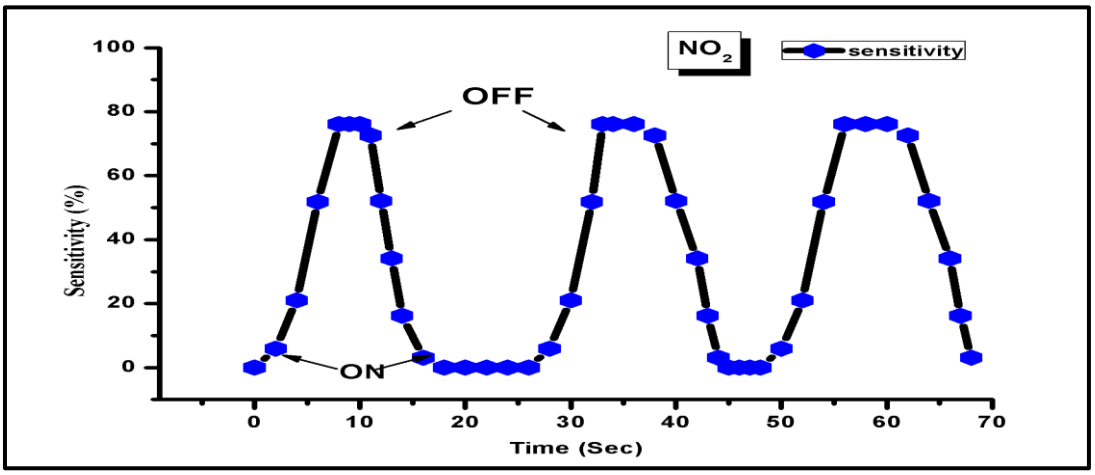

Fig. 8 Response and recovery time of NiO-ZnO thick film for NO_2 gas

5. **NO_2 gas sensing mechanism for NiO-ZnO nanocomposite thick film**

NiO is a p-type metal oxide semiconductor material (MOS). The bulk of charge carriers in p-type semiconductors are positive holes. When the surface of a p-type semiconductor encounters with a reducing gas, resistance rises, implying that resistivity rises because the targeted gas introduces negative charge into the material, lowering the concentration of holes. Because targeted gas interacts with the surface, it increases the concentration of positive holes [1-4]. Due to electrostatic contact generated between oppositely charged species, the adsorption of oxygen anions produces a hole accumulation layer near the surface of MOS in the case of gas sensing mechanism of p-type semiconductor. The surface of the sensing material influences the gas sensing operation. Near the temperature of 100 C, electrons from the valence band of ZnO modified NiO are accelerated from the valence band to the conduction band and are available to interact with adsorbed O_2 species to form reduced O_2^- species. Because the amount of adsorbed oxygen on the surface of the sensing material is proportional to its specific surface area, surface area plays a significant role in the sensing mechanism. Adsorption of large amounts of oxygen species required a wide surface area. In a gaseous environment, a broad charged depletion region occurs across the grain boundaries of ZnO and NiO, resulting in p-n heterojunctions [1, 23, 32]. The electron correlated with this charged species was evacuated from the conduction band of the bulk material, increasing the resistance of film. As a result, a possible barrier appears at the border, prompting a gas response.

Conclusion

The nanocomposites NiO-ZnO thick films with the different weight proportions have been prepared by very conventional, eco-friendly and cost effective screen printing technique. The thick films shows maximum sensitivity to NO_2 gas at low temperature is a prominent property of the developed films. The resistivity and film thickness of NiO-ZnO thick film decreases as additive wt % (ZnO) increase. The TCR found to be negative to all prepared NiO-ZnO thick films shows semiconducting nature of prepared films. XRD results confirmed the formation of NiO-ZnO nanocomposites. The XRD plots matched perfectly with JCPDS card No. 01-075-0197 and JCPDS card No. 00-036-1451 for NiO and ZnO respectively. XRD confirms the ZnO has

hexagonal Wurtzite structure and NiO has Bunsenite face centred cubic (FCC) crystalline structure. FESEM micrographs of NiO-ZnO thick films clearly shows presence of NiO-ZnO nanoparticles on surface. The specific surface area of films was increases with increase wt % ZnO additive in NiO. Energy dispersive analysis (EDAX) spectra shows the film has excess oxygen and also shows that Ni, Zn and O are present in non-stoichiometry ratio. Developed films shows good response and recovery time.

Acknowledgment
The authors are thanks to the Research Centre in Physics, Department of Physics, M.S.G College, Malegaon, district- Nashik, India for providing laboratory facilities. The author also thanks the Department of Physics at Savitribai Phule Pune University, Pune for providing the facilities for SEM, EDAX, XRD, FTIR and UV visible spectroscopy characterization for current research work.

Financial support and sponsorship
Nil.

Conflicts of interest
The authors declare that there are no conflicts of interest regarding the publication of this paper.

References

1. Shinde, V.S., Kapadnis, K.H., Patil, A.P. and Koli, P.B., 2022. Designing of $LaCrO_3$– TiO_2 nanocomposites p: n heterojunction-based sensor material for the selective detection of volatile petrol vapors (PV) and CO2 gas vapors. *Journal of the Indian Chemical Society*, *99*(3), p.100367.
2. Koli, P.B., Kapadnis, K.H. and Deshpande, U.G., 2019. Transition metal decorated Ferrosoferric oxide (Fe_3O_4): An expeditious catalyst for photodegradation of Carbol Fuchsin in environmental remediation. *Journal of Environmental Chemical Engineering*, *7*(5), p.103373.
3. Yang, S., Lei, G., Xu, H., Lan, Z., Wang, Z. and Gu, H., 2021. Metal oxide based heterojunctions for gas sensors: A review. *Nanomaterials*, *11*(4), p.1026.
4. Yang, S., Wang, Z., Hu, Y., Luo, X., Lei, J., Zhou, D., Fei, L., Wang, Y. and Gu, H., 2015. Highly responsive room-temperature hydrogen sensing of α-MoO_3 nanoribbon membranes. *ACS applied materials & interfaces*, *7*(17), pp.9247-9253.
5. Dontsova, T.A., Nahirniak, S.V. and Astrelin, I.M., 2019. Metaloxide nanomaterials and nanocomposites of ecological purpose. *Journal of Nanomaterials*, *2019*.
6. Hassan, A.I. and Yahya, A.M., 2020, March. Structural and optical properties of NiO-ZnO nanocomposite thin film prepared by spray pyrolysis. In *AIP Conference Proceedings* (Vol. 2213, No. 1, p. 020208). AIP Publishing LLC.
7. Zappa, D., Bertuna, A., Comini, E., Kaur, N., Poli, N., Sberveglieri, V. and Sberveglieri, G., 2017. Metal oxide nanostructures: preparation, characterization and functional applications as chemical sensors. *Beilstein journal of nanotechnology*, *8*(1), pp.1205-1217.
8. Yasmeen, S., Iqbal, F., Munawar, T., Nawaz, M.A., Asghar, M. and Hussain, A., 2019. Synthesis, structural and optical analysis of surfactant assisted ZnO–NiO nanocomposites prepared by homogeneous precipitation method. *Ceramics International*, *45*(14), pp.17859-17873.
9. Bouhank, A. and Bellal, Y., 2021. Effect of Different Precursors Solution of NiO on the Properties of ZnO/NiO Nanocomposites Thin Films Grown by Spray Pyrolysis. In *Journal of Nano Research* (Vol. 69, pp. 23-31). Trans Tech Publications Ltd.
10. Sato, H., Minami, T., Takata, S. and Yamada, T., 1993. Transparent conducting p-type NiO thin films prepared by magnetron sputtering. *Thin solid films*, *236*(1-2), pp.27-31.
11. Xuping, Z. and Guoping, C., 1997. The microstructure and electrochromic properties of nickel oxide films deposited with different substrate temperatures. *Thin Solid Films*, *298*(1-2), pp.53-56.
12. Park, C., Kim, J., Lee, K., Oh, S.K., Kang, H.J. and Park, N.S., 2015. Electronic, optical and electrical properties of nickel oxide thin films grown by RF magnetron sputtering. *Applied Science and Convergence Technology*, *24*(3), pp.72-76.
13. Gowthami, V., Meenakshi, M., Perumal, P., Sivakumar, R. and Sanjeeviraja, C., 2014. Optical dispersion characterization of NiO thin films prepared by nebulized spray technique. *Int. J. ChemTech Res*, *6*(13), pp.5196-5202.
14. Ismail, R.A., Ghafori, S.A. and Kadhim, G.A., 2013. Preparation and characterization of nanostructured nickel oxide thin films by spray pyrolysis. *Applied Nanoscience*, *3*(6), pp.509-514.
15. Gomaa, M.M., Yazdi, G.R., Schmidt, S., Boshta, M., Khranovskyy, V., Eriksson, F., Farag, B.S., Osman, M.B.S. and Yakimova, R., 2017. Effect of precursor solutions on the structural and optical properties of sprayed NiO thin films. *Materials Science in Semiconductor Processing*, *64*, pp.32-38.
16. Xu, S. and Wang, Z.L., 2011. One-dimensional ZnO nanostructures: solution growth and functional properties. *Nano Research*, *4*(11), pp.1013-1098.
17. Schmidt-Mende, L. and MacManus-Driscoll, J.L., 2007. ZnO–nanostructures, defects, and devices. *Materials today*, *10*(5), pp.40-48.
18. Kumar, S.S., Venkateswarlu, P., Rao, V.R. and Rao, G.N., 2013. Synthesis, characterization and optical properties of zinc oxide nanoparticles. *International Nano Letters*, *3*(1), pp.1-6.
19. Elemike, E.E., Onwudiwe, D.C. and Singh, M., 2020. Eco-friendly synthesis of copper oxide, zinc oxide and copper oxide–zinc oxide nanocomposites, and their anticancer applications. *Journal of Inorganic and Organometallic Polymers and Materials*, *30*(2), pp.400-409.

20. Parihar, V., Raja, M. and Paulose, R., 2018. A brief review of structural, electrical and electrochemical properties of zinc oxide nanoparticles. *Reviews on Advanced Materials Science*, *53*(2), pp.119-130.
21. Zhang, Z., Shao, C., Li, X., Wang, C., Zhang, M. and Liu, Y., 2010. Electrospun nanofibers of p-type NiO/n-type ZnO heterojunctions with enhanced photocatalytic activity. *ACS applied materials & interfaces*, *2*(10), pp.2915-2923.
22. Sultan, M., Mumtaz, S., Ali, A., Khan, M.Y. and Iqbal, T., 2017. Band alignment and optical response of facile grown NiO/ZnO nano-heterojunctions. *Superlattices and Microstructures*, *112*, pp.210-217.
23. Tupe, U.J., Zambare, M.S., Patil, A.V. and Koli, P.B., 2020. The Binary Oxide NiO-CuO Nanocomposite Based Thick Film Sensor for the Acute Detection of Hydrogen Sulphide Gas Vapours. *Material Science Research India*, *17*(3), pp.260-269.
24. Podesva, P. and Foret, F., 2013. Thin metal films in resistivity-based chemical sensing. *Current analytical chemistry*, *9*(4), pp.642-652.
25. Park, C., Kim, J., Lee, K., Oh, S.K., Kang, H.J. and Park, N.S., 2015. Electronic, optical and electrical properties of nickel oxide thin films grown by RF magnetron sputtering. *Applied Science and Convergence Technology*, *24*(3), pp.72-76.
26. Deore, M.K., Gaikwad, V.B., Patil, R.L., Pawar, N.K., Shinde, S.D. and Jain, G.H., 2010. Effect of Ni doping on gas sensing performance of ZnO thick film resistor. *Sensors & Transducers*, *122*(11), p.143.
27. Miller, D.R., Akbar, S.A. and Morris, P.A., 2014. Nanoscale metal oxide-based heterojunctions for gas sensing: a review. *Sensors and Actuators B: Chemical*, *204*, pp.250-272.
28. Gharbi, B., et al. "Spray pyrolysis synthesized and ZnO–NiO nanostructured thin films analysis with their nanocomposites for waveguiding applications." Semiconductors *55*.1 (2021): 37-43
29. Majumdar, S., 2015. The effects of crystallite size, surface area and morphology on the sensing properties of nanocrystalline SnO2 based system. *Ceramics International*, *41*(10), pp.14350-14358.
30. Saruhan, B., Lontio Fomekong, R. and Nahirniak, S., 2021. Influences of semiconductor metal oxide properties on gas sensing characteristics. *Frontiers in Sensors*, *2*, p.657931.
31. Yousaf, S., Zulfiqar, S., Din, M.I., Agboola, P.O., Aboud, M.F.A., Warsi, M.F. and Shakir, I., 2021. Solar light irradiated photocatalytic activity of ZnO–NiO/rGO nanocatalyst. *Journal of Materials Research and Technology*, *12*, pp.999-1009.
32. Chen, H., Bo, R., Shrestha, A., Xin, B., Nasiri, N., Zhou, J., Di Bernardo, I., Dodd, A., Saunders, M., Lipton-Duffin, J. and White, T., 2018. NiO–ZnO nanoheterojunction networks for room-temperature volatile organic compounds sensing. *Advanced Optical Materials*, *6*(22), p.1800677.